Magnetopolaron in a weakly elliptical InAs/GaAs quantum dot

L. Jacak,[1] J. Krasnyj,[2,*] D. Jacak,[3] and P. Machnikowski[1]
[1]*Institute of Physics, Wrocław University of Technology, Wybrzeże Wyspiańskiego 27, 50-370 Wrocław, Poland*
[2]*Institute of Mathematics, University of Opole, Oleska 48, 45-051 Opole, Poland*
[3]*Institute of Mathematics, Wrocław University of Technology, Wybrzeże Wyspiańskiego 27, 50-370 Wrocław, Poland*
(Received 13 December 2001; revised manuscript received 16 May 2002; published 13 January 2003)

We study theoretically the properties of a polaron formed in a shallow, weakly elliptical, disk-shaped InAs/GaAs quantum dot in the presence of a magnetic field by using the Davydov's canonical transformation. Special attention is paid to the energy-level splitting due to the Fröhlich interaction of an electron in a quantum dot with optical phonons near resonance. The polaron relaxation rates, including the anharmonicity induced channel, are analyzed for various confinement energies and magnetic field magnitudes, taking into account coherent polaronic effects.

DOI: 10.1103/PhysRevB.67.035303 PACS number(s): 73.21.La, 71.38.−k, 03.67.Lx

I. INTRODUCTION

Due to their availability and still growing understanding of their properties, quantum dots (QD's) are believed to be in the center of the imminent technological revolution, e.g., in laser technology[1] or in quantum computing.[2,3] In the latter field, the scalability and integrability of semiconductor systems, as well as the high precision of ultrafast optical techniques,[4] opens the perspective to set up a fully optically driven quantum logic gate based on a QD system.[3] Since the electronic (or excitonic) states in a system of QD's are designed to play the role of qubits which must be manipulated with great precision, exact knowledge of the energetic spectrum of a QD is of major importance. Moreover, because of the necessary quantum coherence during quantum computing processes, the interaction between the localized electron and the surrounding medium must be well understood.

The electronic properties of QD's were widely analyzed.[5] In particular, it has been confirmed that the two-dimensional (2D) harmonic oscillator description for electron states is a relatively good approximation, e.g., in the case of self-assembled InAs/GaAs lens-shaped dots.[6] Since QD's are usually manufactured from polar materials, the electron–longitudinal-optical-phonon interaction must be taken into account in a reliable description. The theoretical investigation of this issue was performed by, e.g., the standard perturbation techniques,[7–9] by the variational Lee-Low-Pines method,[10] by numerical diagonalization,[11,12] or by Green function methods.[13] The experimental data[11] show, in particular, a large splitting width near the one-phonon and two-phonon resonance in a InAs/GaAs QD. This was accounted for by the theoretical model via a numerical diagonalization of the Fröhlich interaction.[11] The required value of the Fröhlich constant seems to be much larger (by a factor of 2,[11] although the most recent results suggest only up to a 25% increase[14]) than measured in bulk. Recently, it was noted that upon the appropriate canonical transformation only a limited number of dispersionless phonon modes (out of an arbitrary number) couple to the electrons, which leads to a considerable simplification of the problem and makes it possible to solve it more efficiently numerically.[12]

In the present paper we propose an entirely analytical nonperturbative technique for solving the electron-phonon eigenvalue problem in a QD in the presence of a magnetic field. This method, based on modification of the Davydov transformation[15,16] appropriate to the localized system, has at least two advantages. First, it may be applied to a system with arbitrary structure of electronic levels and yields explicit approximate formulas for the energetic spectrum in good quantitative agreement with the exact numerical results and with experimental data for an anisotropic QD,[11] both far from and close to the resonances. Second, it employs the description of the system in terms of the well-defined quasiparticles: polarons. The kinetics of the system (e.g., decay rates[17]) may be then easily described including coherent effects.

The paper is organized as follows. In Sec. II we define the model of the QD in a polar medium. Section III contains the approximate analytical diagonalization of the system Hamiltonian by the Davydov method. In Sec. IV, two possible channels of polaron relaxation are discussed. In Sec. V we compare the magnetopolaron spectrum obtained analytically with the exact numerical results. The final section contains a discussion of the results.

II. MODEL

The system under investigation consists of electrons confined in a QD and phonons. Only 3D bulk GaAs phonon modes will be included in the present study. The theoretical analysis[7] shows that for nonspherical dots surface phonon modes may contribute considerably to the shifts in the polaron spectrum. However, we will follow the interpretation proposed in Refs. 11 and 14 and attribute the measured effects only to the bulk modes. The possible influence of other modes requires further clarification which is, however, beyond the scope of this paper. Thus, we take into account longitudinal optical (LO) and longitudinal and transversal acoustical (LA and TA) bulk branches of phonons. The electron-phonon interactions via the LO and LA channels are included as well as the anharmonic third-order LO-TA channel of the phonon interaction (the most efficient phonon anharmonicity in GaAs,[18] the medium of the self-assembled InAs/GaAs quantum dot).

The system is described by the Hamiltonian

$$H=H_{\rm e}(\boldsymbol{r})+\hbar\Omega\sum_{\boldsymbol{k}} b^{\dagger}_{\boldsymbol{k}}b_{\boldsymbol{k}}+\sum_{\boldsymbol{q},s}\hbar\omega_s(\boldsymbol{q})c^{\dagger}_{\boldsymbol{q}s}c_{\boldsymbol{q}s}$$
$$-\frac{1}{\sqrt{N}}\sum_{\boldsymbol{k}}\frac{e}{k}\sqrt{\frac{2\pi\hbar\Omega}{v\tilde{\epsilon}}}(b_{\boldsymbol{k}}+b^{\dagger}_{-\boldsymbol{k}})\exp(i\boldsymbol{k}\cdot\boldsymbol{r})$$
$$+\frac{1}{\sqrt{N}}\sum_{\boldsymbol{q}}\sigma\sqrt{\frac{\hbar q}{2MC_{\rm l}}}(c_{\boldsymbol{q}{\rm l}}+c^{\dagger}_{-\boldsymbol{q}{\rm l}})\exp(i\boldsymbol{q}\cdot\boldsymbol{r})$$
$$+\sum_{\boldsymbol{k}_1,\boldsymbol{k}_2,\boldsymbol{q}}W(\boldsymbol{k}_1,\boldsymbol{k}_2,\boldsymbol{q})\,\delta_{\boldsymbol{k}_1-\boldsymbol{q},\boldsymbol{k}_2}b^{\dagger}_{\boldsymbol{k}_1}b_{\boldsymbol{k}_2}(c_{\boldsymbol{q}{\rm t}}+c^{\dagger}_{-\boldsymbol{q}{\rm t}}),\quad(1)$$

where $b_{\boldsymbol{k}}$ is the bosonic annihilation operator for LO phonons with quasimomentum $\boldsymbol{k}$ and with the dispersionless (for simplicity) frequency Ω, $c_{\boldsymbol{q}s}$ is the bosonic annihilation operator for the acoustical phonon with quasimomentum $\boldsymbol{q}$ and polarization s (t, transversal; l, longitudinal) with frequency $\omega_s(\boldsymbol{q})$, $C_{\rm l}$ is the sound velocity for the longitudinal phonons, M is the mass of ions in the elementary cell, σ is the the deformation potential constant (for GaAs $\sigma\simeq 6$ eV), v is the volume of the elementary cell, N is the number of cells in the crystal, and $\tilde{\epsilon}=(1/\epsilon_\infty-1/\epsilon_0)^{-1}$ is the effective dielectric constant. $H_{\rm e}(\boldsymbol{r})$ is the Hamiltonian for electrons confined in the QD. The electron-LO phonon interaction is given by the Fröhlich term, and the electron-acoustical phonon interaction term includes only LA phonons; the last term describes the third-order anharmonic LO-TA phonon interaction, $W(\boldsymbol{k}_1,\boldsymbol{k}_2,\boldsymbol{q})=W^*(\boldsymbol{k}_2,\boldsymbol{k}_1,-\boldsymbol{q})$.

A. Electron levels in a quantum dot

We will consider the simplified model for the self-assembled, shallow, weakly anisotropic in-plane, InAs/GaAs QD.[11] We will assume that the dot is strongly confined in the z direction (the results do not depend on the actual potential shape in this direction; we assume a strong parabolic confinement). The in-plane electron dynamics is governed by the effective anisotropic harmonic potential $V(x,y)$ with eigenfrequencies $\omega_{\pm}^2=\omega_0^2(1\pm\lambda)$, $\lambda\ll 1$, i.e., $V(x,y)=\frac{1}{2}m^*\omega_0^2(x^2+y^2)+\lambda/2m^*\omega_0^2(x^2-y^2)$. This lateral potential describes the weakly elliptical in-plane QD. The external magnetic field is assumed to be applied in the z direction and described by the potential in the symmetric gauge. Thus, the single-electron Hamiltonian may be written in the cylindrical coordinates $\boldsymbol{r}=(r_\perp\cos\varphi, r_\perp\sin\varphi, z)$ as

$$H_{\rm e}(\boldsymbol{r})=-\frac{\hbar^2}{2m^*}\left[\frac{1}{r_\perp}\frac{\partial}{\partial r_\perp}\left(r_\perp\frac{\partial}{\partial r_\perp}\right)+\frac{1}{r_\perp^2}\frac{\partial^2}{\partial\varphi^2}+\frac{\partial^2}{\partial z^2}\right]$$
$$+\frac{1}{2}m^*\omega^2r_\perp^2+\frac{\hbar\omega_{\rm c}}{2}\left(-i\frac{\partial}{\partial\varphi}\right)+U(z)+W(\boldsymbol{r}_\perp),$$

where $\omega^2=\omega_0^2+\omega_{\rm c}^2/4$, $\omega_{\rm c}=eB/(m^*c)$, $U(z)=\frac{1}{2}m^*\omega_z z^2$, and $\omega_z\gg\omega_0$. The last term, describing the anisotropy,

$$W(\boldsymbol{r}_\perp)=\frac{\lambda}{2}m^*\omega_0^2r_\perp^2\cos 2\varphi,$$

may be treated as a perturbation.

Let us now consider the ground and lowest excited states for the single electron in the dot. For the unperturbed electron Hamiltonian [i.e., neglecting $W(\boldsymbol{r}_\perp)$], we deal with the cylindrical symmetry and thus with the usual n_r and m quantum numbers (the Fock-Darwin states). We consider states with $n_r=0$, $m=0,\pm1$. The energies and wave functions including the perturbation caused by the term W have the following form [we use indices $0,\pm$, for perturbed states (0,0) and $(0,\pm1)$, respectively]:

$$\epsilon_0=\hbar\omega,\quad(2a)$$

$$\Psi_0(\boldsymbol{r})=\psi_0(r_\perp)\phi(z),\quad(2b)$$

$$\epsilon_\pm=2\hbar\omega\pm\hbar\sqrt{\omega_{\rm c}^2+(\lambda\omega_0)^2},\quad(2c)$$

$$\Psi_\pm(\boldsymbol{r})=[c_+\psi_{\pm1}(\boldsymbol{r}_\perp)\pm c_-\psi_{\mp1}(\boldsymbol{r}_\perp)]\phi(z),\quad(2d)$$

where

$$c_\pm=\frac{1}{\sqrt{2}}\left[1\pm\frac{\omega_{\rm c}}{\sqrt{(\lambda\omega_0)^2+\omega_{\rm c}^2}}\right]^{1/2},$$

ψ_0 and $\psi_{\pm1}$ stand for the wave functions for the two-dimensional isotropic harmonic potential,

$$\psi_m(\boldsymbol{r}_\perp)=\sqrt{\frac{n_{\rm r}!}{(n_{\rm r}+|m|)!}}\frac{1}{l_{\rm B}\sqrt{\pi}}\left(\frac{r_\perp}{l_{\rm B}}\right)^{|m|}e^{-(r_\perp/l_{\rm B})^2/2}e^{im\varphi},$$

where $m=0,\pm1$, $l_{\rm B}=\sqrt{\hbar/(m^*\omega)}$, and $\phi(z)$ is the ground-state harmonic oscillator wave function in the z direction (cf. Appendix A).

If we now introduce the second-quantization representation in the electron Hamiltonian $H_{\rm e}(\boldsymbol{r})$, then the entire Hamiltonian (1) can be rewritten as follows:

$$H=H_0+H_1,\quad(3a)$$

$$H_0=\sum_n\epsilon_n a_n^{\dagger}a_n+\hbar\Omega\sum_{\boldsymbol{k}}b^{\dagger}_{\boldsymbol{k}}b_{\boldsymbol{k}}+\sum_{\boldsymbol{q},s}\hbar\omega_s(\boldsymbol{q})c^{\dagger}_{\boldsymbol{q}s}c_{\boldsymbol{q}s}$$
$$+\frac{1}{\sqrt{N}}\sum_{n_1,n_2,\boldsymbol{k}}F^{\rm o}_{n_1n_2}(\boldsymbol{k})a^{\dagger}_{n_1}a_{n_2}(b_{\boldsymbol{k}}+b^{\dagger}_{-\boldsymbol{k}}),\quad(3b)$$

and

$$H_1=\frac{1}{\sqrt{N}}\sum_{n_1,n_2,\boldsymbol{q}}F^{\rm a}_{n_1n_2}(\boldsymbol{q})a^{\dagger}_{n_1}a_{n_2}(c_{\boldsymbol{q}l}+c^{\dagger}_{-\boldsymbol{q}l})$$
$$+\sum_{\boldsymbol{k}_1,\boldsymbol{k}_2,\boldsymbol{q}}W(\boldsymbol{k}_1,\boldsymbol{k}_2,\boldsymbol{q})\,\delta_{\boldsymbol{k}_1-\boldsymbol{q},\boldsymbol{k}_2}b^{\dagger}_{\boldsymbol{k}_1}b_{\boldsymbol{k}_2}(c_{\boldsymbol{q}t}+c^{\dagger}_{-\boldsymbol{q}t}),\quad(3c)$$

where

$$F^{o}_{n_1n_2}(\boldsymbol{k}) = F^{o*}_{n_2n_1}(-\boldsymbol{k}) = -\frac{e}{k}\sqrt{\frac{2\pi\Omega\hbar}{v\tilde{\epsilon}}}\mathcal{F}_{n_1n_2}(\boldsymbol{k}) \tag{4}$$

and

$$F^{a}_{n_1n_2} = \sigma\sqrt{\frac{\hbar q}{2MC_l}}\mathcal{F}_{n_1n_2}(\boldsymbol{k}),$$

with

$$\mathcal{F}_{n_1n_2}(\boldsymbol{k}) = \int d^3r \Psi^*_{n_1}(\boldsymbol{r})\exp(i\boldsymbol{k}\cdot\boldsymbol{r})\Psi_{n_2}(\boldsymbol{r}) \tag{5}$$

(in the above formulas n comprises electron state indices, in our model case $n=0$ or $\pm$).

Note that in the definition of $F^{o}_{n_1n_2}(\boldsymbol{k})$ it is customary to rearrange the coefficients, namely, $F^{o}_{n_1n_2}(\boldsymbol{k}) = [\sqrt{4\pi\alpha}\hbar\Omega(1/\sqrt{vQ_0^3})Q_0/k]\mathcal{F}_{n_1n_2}(\boldsymbol{k})$, where $Q_0 = \sqrt{2m^*\Omega/\hbar}$ and α is the dimensionless Fröhlich constant (cf. Appendix B).

B. Coupling functions

The form factors (5) for the states $\Psi_{0,\pm}$ given by Eqs. (2b) and (2d) are

$$\mathcal{F}_{nn'} = g_{nn'}(k_\perp,\varphi_0)e^{-(k_\perp l_B/2)^2}e^{-(k_z l_z/2)^2}, \tag{6}$$

where $l_z = \sqrt{\hbar/(m^*\omega_z)}$ is the confinement length in the z direction and the functions $g_{nn'}$ are given by the formulas

$$g_{00} = 1,$$

$$g_{0\pm} = -g^*_{\pm 0} = i\xi(c_+e^{\pm i\varphi_0} \pm c_-e^{\mp i\varphi_0}),$$

$$g_{\pm\pm} = 1-\xi^2|c_+e^{i\varphi_0} \pm c_-e^{-i\varphi_0}|^2,$$

$$g_{\pm\mp} = -\xi^2(|c_+|^2e^{-2i\varphi_0} + |c_-|^2e^{2i\varphi_0}) \pm (1-\xi^2)(c^*_-c_+ - c^*_+c_-),$$

where $\xi = k_\perp l_B/2$.

III. ELECTRON–LO-PHONON INTERACTION

A. General description

Due to the interaction between the electron localized in the QD and the LO phonons in the polar medium, the electron is dressed in a polarization cloud, forming a polaron—a superposition of electronic and phononic states. The spectrum of the polaron may be found using the canonical transformation introduced by Davydov and Pestryakov.[15]

This transformation is defined by the unitary operator $\mathsf{U} = e^{\mathsf{S}}$, where S is an anti-Hermitian operator,

$$\mathsf{S}(a,b) = \sum_{n_1,n_2,\boldsymbol{k}} \Phi_{n_1,n_2}(\boldsymbol{k})a^\dagger_{n_1}a_{n_2}(b_{\boldsymbol{k}} - b^\dagger_{-\boldsymbol{k}}), \tag{7}$$

with the scalar function

$$\Phi_{n_1,n_2}(\boldsymbol{k}) = \Phi^*_{n_2,n_1}(-\boldsymbol{k})$$

chosen suitably for the diagonalization demands. The Hamiltonian H_0 [Eq. (3b)] may be written as

$$H_0(a,b) = \mathsf{U}^\dagger[\mathsf{U}H_0\mathsf{U}^\dagger]\mathsf{U} = \mathsf{U}^\dagger H_0(\alpha,\beta)\mathsf{U},$$

where $H_0(\alpha,\beta)$ is H_0 Hamiltonian with the operators a, b replaced by operators $\alpha = \mathsf{U}a\mathsf{U}^\dagger$, $\beta = \mathsf{U}b\mathsf{U}^\dagger$, respectively [note that $U(a,b) = U(\alpha,\beta)$].

The generator S (i.e., the function Φ) may be chosen in such a way that $\mathsf{U}^\dagger H(\alpha,\beta)\mathsf{U}$ does not contain terms linear in β. Indeed, neglecting residual multipolaron and multiphonon interaction terms[15,16] (these terms are of higher order in the Fröhlich constant, $\alpha \ll 1$, and thus are small),

$$\begin{aligned} e^{-\mathsf{S}}H_0(\alpha,\beta)e^{\mathsf{S}} \approx{}& \sum_n E_n\alpha^\dagger_n\alpha_n + \hbar\Omega\sum_{\boldsymbol{k}}\beta^\dagger_{\boldsymbol{k}}\beta_{\boldsymbol{k}} + \sum_{\boldsymbol{q},s}\hbar\omega_s(\boldsymbol{q})c^\dagger_{\boldsymbol{q}s}c_{\boldsymbol{q}s} \\ &+ \sum_{n_1,n_2,\boldsymbol{k}}\Bigg\{\Bigg[-\Phi_{n_1n_2}(\boldsymbol{k})(\epsilon_{n_2}-\epsilon_{n_1}+\hbar\Omega) \\ &+ \frac{1}{2}\sum_{n_3}[\Phi_{n_1n_3}(\boldsymbol{k})D_{n_3n_2} - \Phi_{n_3,n_2}(\boldsymbol{k})D_{n_3n_1}] \\ &+ \frac{1}{\sqrt{N}}F^{o}_{n_1n_2}(\boldsymbol{k})\Bigg]\alpha^\dagger_{n_1}\alpha_{n_2}\beta_{\boldsymbol{k}} + \text{H.c.}\Bigg\}, \end{aligned} \tag{8}$$

with

$$E_n = \epsilon_n - D_{nn} + \sum_{n_3,\boldsymbol{k}}\Phi_{nn_3}(-\boldsymbol{k})\Phi_{n_3n}(\boldsymbol{k})(\epsilon_{n_3}-\epsilon_n+\hbar\Omega) \tag{9}$$

and

$$D_{n_1n_2} = \frac{1}{\sqrt{N}}\sum_{n_3,\boldsymbol{k}}[\Phi_{n_1n_3}(\boldsymbol{k})F^{o}_{n_3n_2}(-\boldsymbol{k}) + \Phi_{n_3n_1}(\boldsymbol{k})F^{o}_{n_2n_3}(-\boldsymbol{k})]. \tag{10}$$

The requirement that the coefficient at the term linear in β should vanish leads to the equation for Φ,

$$\Phi_{n_1n_2}(\boldsymbol{k}) = \frac{1}{\sqrt{N}}\frac{F^{o}_{n_1n_2}(\boldsymbol{k})}{\epsilon_{n_2}-\epsilon_{n_1}+\hbar\Omega} + \frac{\frac{1}{2}\sum_{n_3}[\Phi_{n_1n_3}(\boldsymbol{k})D_{n_3n_2} - \Phi_{n_3,n_2}(\boldsymbol{k})D_{n_3n_1}]}{\epsilon_{n_2}-\epsilon_{n_1}+\hbar\Omega}. \tag{11}$$

The solution of the above equation in a perturbative manner leads to the known perturbative formula for the polaron energy. Indeed, in the first approximation one has

$$\Phi^{(0)}_{n_1 n_2}(\boldsymbol{k}) = \frac{1}{\sqrt{N}} \frac{F^{o}_{n_1 n_2}(\boldsymbol{k})}{\epsilon_{n_2} - \epsilon_{n_1} + \hbar\Omega}, \tag{12}$$

and from Eqs. (9) and (10), within this approximation,

$$E_n = \epsilon_n - \frac{1}{N} \sum_{n'} \frac{\sum_{\boldsymbol{k}} |F^{o}_{nn'}(\boldsymbol{k})|^2}{\epsilon_{n'} - \epsilon_n + \hbar\Omega}. \tag{13}$$

This approximation breaks down in a wide range of the magnetic fields around the resonances.

To improve this solution we use the fact that $D_{nn'}$ decreases rapidly as $|n-n'|$ grows, and then

$$\Phi_{n_1 n_2}(\boldsymbol{k}) \approx \frac{1}{\sqrt{N}} \frac{F^{o}_{n_1 n_2}(\boldsymbol{k})}{\epsilon_{n_2} - \epsilon_{n_1} + \hbar\Omega} + \frac{\frac{1}{2}\Phi_{n_1 n_2}(\boldsymbol{k})(D_{n_2 n_2} - D_{n_1 n_1})}{\epsilon_{n_2} - \epsilon_{n_1} + \hbar\Omega}.$$

Using further the zeroth order approximation $\Phi^{(0)}_{n_1 n_2}(\boldsymbol{k})$ only under the sum in Eq. (9) for E_n, we arrive at the following solutions:

$$E_n = \epsilon_n - \frac{1}{2} D_{nn} \tag{14}$$

and, instead of Eq. (12),

$$\Phi_{n_1 n_2}(\boldsymbol{k}) = \frac{1}{\sqrt{N}} \frac{F^{o}_{n_1 n_2}(\boldsymbol{k})}{E_{n_2} - E_{n_1} + \hbar\Omega}. \tag{15}$$

Taking into account the formula for D_{nn}, Eq. (14) resolves finally into

$$E_n = \epsilon_n - \sum_{n'} \frac{J_{n'n}}{E_{n'} - E_n + \hbar\Omega}, \tag{16}$$

where

$$J_{n'n} = \frac{1}{N} \sum_{\boldsymbol{k}} |F^{o}_{n'n}(\boldsymbol{k})|^2.$$

The above equation (16) is the self-consistent nonperturbative equation for the energy E_n of the polaron, originally applied for bulk semiconductor by Davydov and Pestryakov.

Note also that in our case of the electron confined in the QD, similarly as for an unconfined electron,[16] the polaron states are highly distinct from the original electron states, while the phonon states are almost not modified by coherent effects. This follows from the formulas

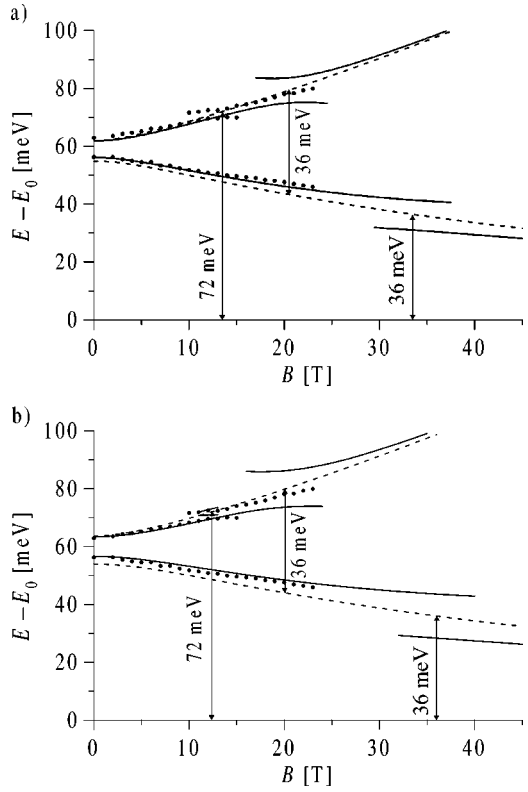

FIG. 1. Polaron resonances in a weakly elliptical quantum dot in the presence of a magnetic field for (a) $\alpha = 0.07$ and (b) $\alpha = 0.15$ (the other system parameters are given in the Sec. III A). The shifted polaron levels $E^{(1)}_n(\boldsymbol{B}) - E^{(1)}_0(\boldsymbol{B})$, Eq. (17) (dashed lines), branches of polaron levels split in the vicinity of resonances $E_n(\boldsymbol{B}) - E_0(\boldsymbol{B})$ (solid lines), and the experimental data after Ref. 11 (dots).

$$\alpha^{\dagger}_n|0\rangle \simeq a^{\dagger}_n|0\rangle - \frac{1}{2} \sum_{n_1, n_2, \boldsymbol{k}} \Phi_{n_1 n}(\boldsymbol{k}) \Phi_{n_2 n_1}(-\boldsymbol{k}) a_{n_2}|0\rangle - \sum_{n_1, \boldsymbol{k}} \Phi_{n_1 n}(-\boldsymbol{k}) b^{\dagger}_{\boldsymbol{k}} a^{\dagger}_{n_1}|0\rangle$$

and

$$\beta^{\dagger}_{\boldsymbol{k}}|0\rangle \simeq b^{\dagger}_{\boldsymbol{k}}|0\rangle$$

(the vacuum state $|0\rangle$ is defined by formulas: $\Psi_0 = a^{\dagger}_0|0\rangle$ and $a_n\Psi_0 = b_{\boldsymbol{k}}\Psi_0 = c_{\boldsymbol{q},s}\Psi_0 = 0$ for all $\boldsymbol{k}$, $\boldsymbol{q}$ and $n \neq 0$).

Let us denote for future convenience

$$E^{(1)}_n = \epsilon_n - \frac{1}{\hbar\Omega} J_{nn}. \tag{17}$$

These entities are the Huang-Rhys approximations to the polaron energy levels,[19] but they are insensitive to polaron-phonon resonances (cf. Fig. 1).

The factors $J_{nn'}$ in the harmonic approximation are

$$J_{nn'} = j_{nn'} \frac{\sqrt{\pi}}{2} \alpha \hbar^2 \Omega \sqrt{\omega\Omega}, \tag{18}$$

where the values of the coefficients $j_{nn'}$ for the weakly elliptical quantum dot in a magnetic field are given as

n	0	+	−
0	1	$\frac{1}{4}$	$\frac{1}{4}$
+	$\frac{1}{4}$	$\frac{11}{16}+\frac{3}{8}\lvert c_+c_-\rvert^2$	$\frac{3}{16}-\frac{5}{8}\lvert c_+c_-\rvert^2$
−	$\frac{1}{4}$	$\frac{3}{16}-\frac{5}{8}\lvert c_+c_-\rvert^2$	$\frac{11}{16}+\frac{3}{8}\lvert c_+c_-\rvert^2$

For the InAs/GaAs dot, with $\hbar\Omega\simeq 36$ meV, $\hbar\omega_0 \simeq 58$ meV, and $\alpha\sim 0.1$ we have

$$\frac{J_{nn'}}{(\hbar\Omega)^2}\ll 1,$$

which highly simplifies the further analysis.

First, let us consider the nonresonant situation, i.e.,

$$E_n^{(1)}-E_{n'}^{(1)}-\hbar\Omega\sim\hbar\Omega.$$

In this case the eigenvalues E_n differ only slightly from $E_n^{(1)}$ and one can replace the former with the latter in the denominator of Eq. (16). Thus, outside the resonance region we have

$$E_n\approx E_n^{(1)}+\sum_{n'\neq n}\frac{J_{nn'}}{E_n^{(1)}-E_{n'}^{(1)}-\hbar\Omega}.$$

We will now proceed to the examination of Eq. (16) near the one-phonon resonance between the levels n_1 and n_2, $E_{n_1}^{(1)}-E_{n_2}^{(1)}-\hbar\Omega=0$, i.e., in the case of

$$\epsilon_{n_1}-\epsilon_{n_2}-\hbar\Omega\sim\sqrt{J_{n_1n_2}}\ll\hbar\Omega. \tag{19}$$

Let us introduce the following notation for the energy level shifts: $\Delta E_n=E_n-E_n^{(1)}$, $\Delta E_{n_1n_2}=\Delta E_{n_1}-\Delta E_{n_2}$, and $E_{n_1n_2}=\frac{1}{2}(\Delta E_{n_1}+\Delta E_{n_2})$. Then we find from the self-consistent equation (16)

$$\Delta E_{n_1n_2}=\frac{J_{n_1n_2}}{\Delta E_{n_1n_2}+f_{n_1n_2}}-\frac{J_{n_1n_2}}{-\Delta E_{n_1n_2}+f_{n_2n_1}} +\sum_{n'\neq n_1,n_2}\left(\frac{J_{n_1n'}}{\Delta E_{n_1n'}+f_{n_1n'}}-\frac{J_{n_2n'}}{\Delta E_{n_2n'}+f_{n_2n'}}\right),$$

where $f_{n_1n_2}=E_{n_1}^{(1)}-E_{n_2}^{(1)}-\hbar\Omega$. As $\lvert f_{n_2n_1}\rvert\simeq 2\hbar\Omega\gg\sqrt{J_{n_1n_2}}$, $\lvert f_{n_1n_2}\rvert\simeq 0$ (near the resonance) and $\lvert f_{n_1n'}\rvert\sim\lvert f_{n_2n'}\rvert\sim\hbar\Omega \gg\sqrt{J_{n_{1,2}n'}}$, then

$$\Delta E_{n_1n_2}\simeq\frac{J_{n_1n_2}}{\Delta E_{n_1n_2}+f_{n_1n_2}}.$$

The above equation has the simple solution

$$\Delta E_{n_1n_2}^{\pm}=-f_{n_1n_2}/2\pm\sqrt{(f_{n_1n_2}/2)^2+J_{n_1n_2}}$$

[at the resonance point, given by Eq. (19), $f_{n_1n_2}=0$]. The $\pm$ pair of the solutions corresponds to the usual splitting of the polaron energy near the resonance. In order to find E_{n_1} and E_{n_2} it is necessary to find also $E_{n_1n_2}$ via solution of the equation

$$E_{n_1n_2}=\frac{1}{2}\left(\frac{J_{n_1n_2}}{\Delta E_{n_1n_2}+f_{n_1n_2}}+\frac{J_{n_1n_2}}{-\Delta E_{n_1n_2}+f_{n_2n_1}}\right) +\frac{1}{2}\sum_{n'\neq n_1,n_2}\left(\frac{J_{n_1n'}}{\Delta E_{n_1n'}+f_{n_1n'}}+\frac{J_{n_2n'}}{\Delta E_{n_2n'}+f_{n_2n'}}\right).$$

From this equation one finds

$$E_{n_1n_2}\simeq\frac{1}{2}\Delta E_{n_1n_2}+\Delta E_{n_1n_2}\frac{J_{n_1n_2}}{(2\hbar\Omega)^2}+\frac{J_{n_1n_2}}{2\hbar\Omega} +\sum_{n'\neq n_1,n_2}\frac{J_{n_2n'}}{\Delta E_{n_2n'}+f_{n_2n'}}.$$

The splittings for both states are

$$\Delta E_{n_1}^{+}-\Delta E_{n_1}^{-}=2\sqrt{(f_{n_1n_2}/2)^2+J_{n_1n_2}} \tag{20a}$$

and

$$\Delta E_{n_2}^{+}-\Delta E_{n_2}^{-}=2\frac{J_{n_1n_2}}{(2\hbar\Omega)^2}\sqrt{(f_{n_1n_2}/2)^2+J_{n_1n_2}}. \tag{20b}$$

We see that only the upper state (i.e., n_1, since $E_{n_1}>E_{n_2}$) splits. The splitting of the lower one has to be neglected due to the small factor $J_{n_1n_2}/(2\hbar\Omega)^2$.

B. Application to the dot model and comparison with experiment

We are going to study in more detail the polaronic resonances in a model of a weakly elliptical dot as described in Sec. II A (in analogy to the dot examined experimentally[11]). A quantum dot is a strongly inhomogeneous system: both electronic and phononic parameters of InAs differ from those of GaAs. Moreover, a real quantum dot is a complex system, where the electronic spectrum, primarily defined by the spatial confinement, is affected by shape irregularity, inhomogeneous InAs-GaAs composition[20] or strain-induced band shifts and effective mass modification.[21,22]

On the other hand, within the presented description, the electronic properties of the dot enter the electron-phonon coupling only via the form factors $\mathcal{F}_{nn'}(\boldsymbol{k})$ [Eq. (5)], which depend on the wave function shape. In particular, it has been verified[17] that modification of the confinement potential shape does not influence significantly the polaron spectrum and the relaxation rates. Therefore, it seems reasonable to simplify the analysis by using the effective model with the simplest, harmonic-oscillator approximation for the wave functions, which results in only one parameter (localization width l_B or potential strength ω_0) to be adjusted based on the

experiment. The resulting incompatibility between the coupling strength and the confined electron eigenenergies may be accounted for by choosing a modified, effective value of the Fröhlich constant α. It has been reported recently[14] that the necessary correction does not exceed 25%.

The presence of strain-induced, self-assembled InAs dot in the GaAs crystal modifies its phonon spectrum and may lead to the appearance of localized or surface phonon states of the strained InAs nanocrystal. Not much is known about the properties of these modes for a realistic dot shape. However, experimentally measured polaron spectra[11,14] show only strong resonances related to the bulk GaAs LO phonons which suggests that the GaAs surrounding medium phonons are dominant and rather weakly affected by dot nanocrystal structure. Therefore, in the following, we take into account only the bulk GaAs phonon modes with frequency $\hbar\Omega = 36$ meV (dispersion is neglected except for phonon-phonon coupling constant estimation in the next section). In the present paper we use the model with harmonic lateral confinement, treating the confinement strength as a phenomenological, effective parameter. It was verified[17] that other confinement models do not lead to a considerable modification of the results.

In the simplified, harmonic approximation, the electron spectrum is determined by the values of $\hbar\omega_0$ and λ which may be found by fitting the energy levels E_+ and E_- to their values at $B=0$ measured in the experiment.[11] It is known that the electron effective mass in a strained InAs/GaAs dot becomes close to the GaAs mass.[21] We will use the GaAs mass in our calculation. We use two alternative values of the Fröhlich constant: the bulk one $\alpha=0.07$ and the increased value suggested in Ref. 11, $\alpha=0.15$. This increased value may be explained in phenomenological, semiclassical terms and it may actually account for effects which are not explicitly included in our model Hamiltonian, like piezoelectricity or nonadiabaticity (cf. Appendix B).

Fitting to the experimental results of Ref. 11 leads to the potential parameters $\hbar\omega_0=57.8$, $\lambda=0.122$ and $\hbar\omega_0=57.5$, $\lambda=0.169$ for $\alpha=0.07$ and $\alpha=0.15$, respectively.

Let us first focus on the resonance condition

$$E_-^{(1)}-E_0^{(1)}-\hbar\Omega=0.$$

The corresponding magnetic field B_1 may be found using the definition (17) and the values for the $J_{nn'}$ factors given by Eq. (18). The separation between the branches of the splitting at the resonance point is, according to Eq. (20),

$$\delta E_- = \Delta E_-^+ - \Delta E_-^- = \sqrt{J_{-0}}$$

(the corresponding values are collected in the Table I).

Another possible resonance takes place when

$$E_+^{(1)}-E_-^{(1)}-\hbar\Omega=0.$$

The corresponding magnetic field B_2 is found in a similar way as previously and the separation between the branches at the resonance point is

$$\delta E_+ = \Delta E_+^+ - \Delta E_+^- = \sqrt{J_{+-}}$$

TABLE I. The values of the magnetic fields and the corresponding values of the resonance energy splitting for two parameter sets of the model InAs/GaAs dot.

α	0.07 ($\hbar\omega_0=57.5$ meV, $\lambda=0.122$)	0.15 ($\hbar\omega_0=57.8$ meV, $\lambda=0.169$)
B_1	34 T	36 T
δE_-	10 meV	15 meV
B_2	21 T	20 T
δE_+	9 meV	13 meV
B_3	14 T	12 T
$\delta^{(2)}E_+$	1 meV	2 meV

(cf. Table I).

Apart from the splitting of the "+" state due to one-phonon resonance with the "−" state, there should be another effect, related to two-phonon resonance with the ground state, occurring around the intersection of the zero-phonon E_+ energy level and the $E_0+2\hbar\Omega$ energy corresponding to the ground electron state with two phonons.[11] Actually, one should not expect an exact result here, since some two-phonon terms were neglected in the derivation of Eq. (16). Nevertheless, the presented analytical method allows for an approximate determination of this resonance. Within the zeroth order approximation for this second-order resonance we can write

$$\Delta E_{+0}=\Delta E_+ - \Delta E_0 = \Delta E_{+-} + \Delta E_{-0},$$

and then

$$\Delta E_{+0} = -\frac{f_{+-}+f_{-0}}{2} \pm [\sqrt{(f_{+-}/2)^2+J_{+-}} \pm \sqrt{(f_{-0}/2)^2+J_{-0}}].$$

If we consider only splitting of the "+" state [i.e., the $E_+^{(1)}(B)$ energy] the first term in the above formula has to vanish, i.e., $f_{+-}+f_{-0}=E_+^{(1)}(B_3)-E_0^{(1)}(B_3)-2\hbar\Omega=0$ (it is interesting that this condition is the same as the two-phonon resonance condition for the "+" and "0" states). Taking into account this last condition we find the smallest gap at B_3:

$$\delta^{(2)}E_+ \sim 2|\sqrt{(f_{+-}/2)^2+J_{+-}} - \sqrt{(f_{+-}/2)^2+J_{-0}}|,$$

(cf. Table I).

The spectrum of the system for the two sets of parameters is depicted in Fig. 1 and compared with the experimental results.[11] The agreement for the E_- level is very good. The theoretical curve for E_+ differs from the experiment at high magnetic field which suggests that the theoretical result for the resonance at 20 T is slightly shifted with respect to its actual position (recently determined experimentally[14]). The estimated value of the small splitting at the second-order resonance [shown only in Fig. 1(a)] is also comparable to the experimental value. However, the value obtained for $\alpha=0.07$ is twice as small as the experimental one (as could be expected from the zeroth-order approximation).

IV. POLARON DECAY RATES

Apart from the system spectrum, the Davydov transformation allows also for a convenient description of the relaxation processes, including the coherent polaronic effects. In this section we discuss two channels of polaron relaxation and calculate the relaxation rates for a polaron in a dot in the presence of magnetic field.

Let us study the second term in the Hamiltonian (3a), i.e., H_1 [Eq. (3c)], responsible for the electron–LA-phonon interaction and for the anharmonic phonon decay. Upon the canonical transformation e^{S} the two terms of H_1 attain the following form:

$$H_1=\frac{1}{\sqrt{N}}\sum_{n_1n_2,\boldsymbol{q}} F^{\mathrm{a}}_{n_1n_2}(\boldsymbol{q})\alpha^{\dagger}_{n_1}\alpha_{n_2}(c_{\mathrm{l},\boldsymbol{q}}+c^{\dagger}_{\mathrm{l},-\boldsymbol{q}}) + \sum_{\boldsymbol{k}_1,\boldsymbol{k}_2,\boldsymbol{q}} W(\boldsymbol{k}_1,\boldsymbol{k}_2,\boldsymbol{q})\,\delta_{\boldsymbol{k}_1,\boldsymbol{k}_2+\boldsymbol{q}}\beta^{\dagger}_{\boldsymbol{k}_1}\beta_{\boldsymbol{k}_2}(c_{\mathrm{t},\boldsymbol{q}}+c^{\dagger}_{\mathrm{t},-\boldsymbol{q}}) + \sum_{n_1n_2,\boldsymbol{q},\boldsymbol{k},s}\tilde{W}^{s}_{n_1n_2}(\boldsymbol{q},\boldsymbol{k})\alpha^{\dagger}_{n_1}\alpha_{n_2}\beta_{\boldsymbol{k}}(c_{s,\boldsymbol{q}}+c^{\dagger}_{s,\boldsymbol{q}})+\mathrm{H.c.}, \tag{21}$$

where $s=\mathrm{l,t}$ denotes polarization, as previously, and

$$\tilde{W}^{\mathrm{t}}_{n_1n_2}(\boldsymbol{q},\boldsymbol{k})=-\frac{1}{\sqrt{N}}\frac{F^{\mathrm{o}}_{n_1n_2}(\boldsymbol{k}+\boldsymbol{q})W(\boldsymbol{k}+\boldsymbol{q},\boldsymbol{k},\boldsymbol{q})}{E_{n_2}-E_{n_1}+\hbar\Omega}, \tag{22}$$

$$\tilde{W}^{\mathrm{l}}_{n_1n_2}(\boldsymbol{q},\boldsymbol{k})=-\frac{1}{N}\sum_{n_3}\left[\frac{F^{\mathrm{o}}_{n_1n_3}(\boldsymbol{k})F^{\mathrm{a}}_{n_3n_2}(\boldsymbol{q})}{E_{n_3}-E_{n_1}+\hbar\Omega} - \frac{F^{\mathrm{o}}_{n_3n_2}(\boldsymbol{k})F^{\mathrm{a}}_{n_1n_3}(\boldsymbol{q})}{E_{n_2}-E_{n_3}+\hbar\Omega}\right]. \tag{23}$$

The first term in the transformed Hamiltonian H_1, Eq. (21), describes the polaron–LA-phonon interaction (note that it has the same coupling energy as it was for electron–LA-phonon interaction), and the second term describes anharmonic interaction of LO phonons (almost unaffected by the canonical transformation) with TA phonons (again with the same energy as without the coherent effects), whereas thelast term describes the relaxation of the polaron. The LO-TA anharmonicity-induced relaxation channel corresponds to Eq. (22)while the LO-LA channel to Eq. (23). Note that in the former case [Eq. (22)], the coupling $F^{\mathrm{o}}_{nn'}(\boldsymbol{k}+\boldsymbol{q})$ selects processes with opposite wave vectors $\boldsymbol{k}$ and $\boldsymbol{q}$ [cf. Eqs. (4) and (6)].

Both these channels lead to a change of the polaron state accompanied by the creation or annihilation of a pair of phonons: the optical and one acoustical. There are four possibilities for this process with probabilities (according to the Fermi golden rule)

$$w^{x,y;s}_{n_1n_2}(\boldsymbol{q},\boldsymbol{k})=\frac{2\pi}{\hbar}|\tilde{W}^{s}(n_1n_2,(x\cdot y)\boldsymbol{q},\boldsymbol{k})|^2(N_{\boldsymbol{k}}+\eta_x) \times(\nu_{s,\boldsymbol{q}}+\eta_y)\,\delta(E_{n_1}-E_{n_2}-x\hbar\Omega-y\hbar\omega_{s,\boldsymbol{q}}),$$

where x $(y)=\pm$ and "+" corresponds to emission and "−" to absorption of an optical (acoustical) phonon, respectively, and $\eta_+=1$, $\eta_-=0$ ($N_{\boldsymbol{k}}$, number of LO phonons in the $\boldsymbol{k}$ state; $\nu_{\boldsymbol{q},s}$, number of acoustical phonons in the state $\boldsymbol{q}$ and polarization s).

At sufficiently low temperatures [for GaAs practically at $T<11$ K (Ref. 18)], the phonon occupation numbers are negligible and the only contribution is from the process of the polaron transition with simultaneous emission of two phonons; the corresponding probability is $w^{++}_{n1,n2}(\boldsymbol{q},\boldsymbol{k})$. The relaxation probability for this process is given by the sum

$$w_{n_1\to n_2}=\sum_{\boldsymbol{k},\boldsymbol{q}} w^{++}_{n_1n_2}(\boldsymbol{q},\boldsymbol{k}).$$

The dependence of the amplitude $W(\boldsymbol{k}_1,\boldsymbol{k}_2,\boldsymbol{q})$ on the wave vectors may be established by a general argument.[23] Namely, the long-wavelength acoustic phonons correspond to sound waves, whose elastic energy is expressed in terms of the strain tensor elements, i.e., to the spatial derivatives of the deformation. This dependence leads, in the second-quantization picture, to the linear dependence on the acoustic phonon wave vectors. Hence, the corresponding part of the Hamiltonian, i.e., the probability for a third-order phonon-phonon process with one long-wavelength acoustical phonon involved, must be proportional to the phonon wave number. As an approximation, we extend this dependence over the whole range of q and write

$$|W(\boldsymbol{k}+\boldsymbol{q},\boldsymbol{k},\boldsymbol{q})|^2=\frac{\gamma^2}{N}q,$$

where we also assume that γ weakly depends on the LO phonon wave vector $\boldsymbol{k}$.

Thus, the relaxation probability via the LO-TA channel may be written as

$$w^{(\mathrm{t})}_{n_1\to n_2}=\frac{2}{\pi}\frac{J_{n_1n_2}\gamma^2q_{\mathrm{t}}v}{\hbar^4C^3_{\mathrm{t}}}, \tag{24}$$

where C_{t} is the sound velocity for the transversal phonons and $q_{\mathrm{t}}=(E_{n_1}-E_{n_2}-\hbar\Omega)/\hbar C_{\mathrm{t}}$ (limited by the maximum frequency for TA phonons).

Let us now estimate the polaron relaxation rate for this anharmonicity-induced LO-TA channel. We restrict ourselves to the polaron relaxation from the "−" state to the ground state "0." For the LO-TA process at low temperatures only phonon emission is possible. Energy conservation restricts this process to a certain energy range, related to the maximum energy of the TA phonon, ~ 8 meV (indicated by the dotted lines in Fig. 2). Thus, this channel of polaron relaxation is ineffective for magnetic fields $B<25$ T and $B<33$ T for $\alpha=0.07$ and $\alpha=0.15$, respectively. This situation is characteristic of a dot with the confinement energy $\hbar\omega_0$ exceeding the phonon energy $\hbar\Omega$ by several meV. For comparison, the same two branches of the first excited state at $B=0$ for various dot confinements are shown in the inset in Fig. 2. The relaxation channel by the LO+TA phonon emission from the physically important, stable polaronic branch is

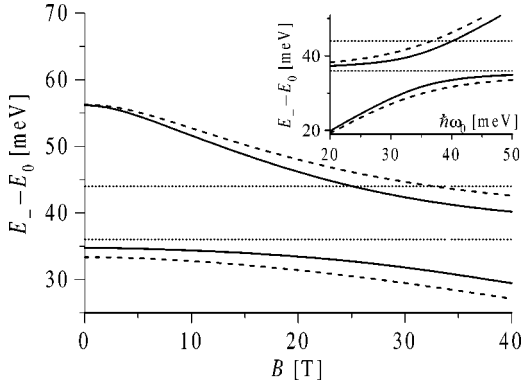

FIG. 2. Two branches of the $E_- - E_0$ polaron energy difference compared with the energy sector where the LO-TA polaron relaxation is possible (shown by dotted lines) ($T=0$) for $\alpha=0.07$ (solid lines) and $\alpha=0.15$ (dashed lines) (see Sec. III B for other system parameters). Inset: the same two branches at $B=0$ for various confinement energies $\hbar\omega_0$.

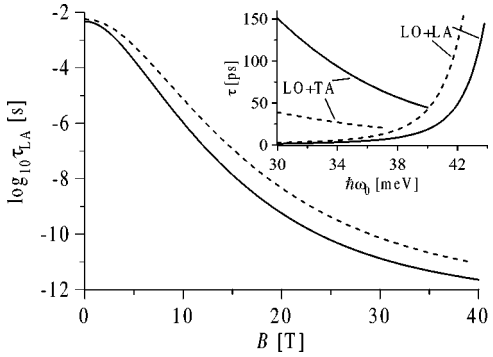

FIG. 3. Polaron relaxation time from the "$-$" level with respect to the LO-LA emission ($T=0$) for $\alpha=0.07$ (solid lines) and $\alpha=0.15$ (dashed lines). Inset: relaxation times with respect to the LO-TA anharmonicity induced channel and to the LO-LA channel for various dots at $B=0$. For strong confinements the LO-TA channel is forbidden by energy conservation.

allowed only if $\hbar\omega_0<40$ meV. Similarly, the process with TA phonon absorption at nonzero temperatures is also possible only in a relatively narrow sector of confinement energies.

For a quantitative estimation of the corresponding relaxation rate the value of the anharmonic phonon-phonon coupling constant is needed; it can be fitted using the experimental data for GaAs bulk.[18] In this estimation, the exact form of the phonon dispersion curves, including the LO phonon dispersion $\Omega(\boldsymbol{k})$, is essential. For GaAs, the dominant anharmonic process involves TA phonons with $\boldsymbol{q}$ in the vicinity of the L point in the Brillouin zone.[18] At low temperatures, for GaAs bulk, we find for the LO phonon lifetime

$$\tau_{\mathrm{LO}}=w^{-1}=\frac{\pi\hbar^2\tilde{c}}{\gamma^2 v q_0^3\mu},$$

where the factor μ accounts for anisotropy effects and q_0 corresponds to the vicinity of the L point. From the experimental data for phonon dispersions in GaAs,[24] one can notice that the energy conservation needed for the considered channel of LO phonon decay is satisfied along the L-W line on the hexagonal zone wall but it is violated towards the Σ line. It therefore seems reasonable to assume that $\mu\approx 0.4$. From the phonon dispersion curves it also results that on the Γ-L line near the L point one has the group velocity of longitudinal phonons $\tilde{c}\approx 0.6C_t$. Using the lifetime $\tau_{\mathrm{LO}}=9.2$ ps at $T=6$ K reported in Ref. 18, one can thus estimate the γ factor. Using this value, the lifetime for the polaron in a GaAs self-assembled quantum dot with respect to the LO-TA relaxation channel can be estimated [at $T=0$ K, according to Eq. (24)]. The polaron relaxation times obtained in this way are of order of 10 ps but for a dot with $\hbar\omega\approx 60$ meV the process is allowed only in the region of very high magnetic fields (cf. Fig. 2).

The LO-LA channel may be responsible for polaron relaxation in a wider range of magnetic fields due to the much higher energies of the LA phonons in GaAs [up to 24 meV (Ref. 24)]. The probability of relaxation has the form [retaining only the largest terms in $\tilde{W}^{\mathrm{l}}_{n_1n_2}(\boldsymbol{q},\boldsymbol{k})$]:

$$w^{(\mathrm{l})}_{n_1\to n_2}=\frac{\sigma^2 J_{n_1n_2}}{4\pi\varrho\hbar^3 C_{\mathrm{l}}^4 q_{\mathrm{l}} l_{\mathrm{B}}^2}\mathcal{J}_{n_1n_2}, \tag{25}$$

where $q_{\mathrm{l}}=(E_{n_1}-E_{n_2}-\hbar\Omega)/\hbar C_{\mathrm{l}}$ (limited by the maximum frequency for LA phonons) and

$$\mathcal{J}_{n_1n_2}=l_{\mathrm{B}}^2\int d^3\boldsymbol{q}\,|\mathcal{F}_{n_2n_2}(\boldsymbol{q})-\mathcal{F}_{n_1n_1}(\boldsymbol{q})|^2\,\delta(q-q_{\mathrm{l}}).$$

For the initial state "$-$" and the final state "0" one has

$$\mathcal{J}_{-0}=(1+2|c_+c_-|^2)\frac{(q_{\mathrm{l}}l_{\mathrm{B}})^6}{15}\times M\left(3,\frac{7}{2},-\frac{1}{2}(l_{\mathrm{B}}^2-l_z^2)q_{\mathrm{l}}^2\right)e^{-(q_{\mathrm{l}}l_z)^2/2}, \tag{26}$$

where M is the degenerated hypergeometric function.[25]

The polaron relaxation time with respect to the LO-LA channel for various magnetic fields and dot sizes is plotted in Fig. 3. It is clear that for the self-assembled dot discussed here, with $\hbar\omega_0\simeq 58$ meV, the initial state is very long living for any practically attainable magnetic field. This is due to the well-known bottleneck mechanism,[26] where the emission of short-wavelength phonons is strongly suppressed in a confined system. It is essential to note that, unlike the bare electronic levels, the polaronic energy levels never approach the resonant LO phonon energy (anticrossing effect). The combined LO-LA phonon emission and absorption is therefore less probable than that obtained by the perturbation theory methods[27,28] and the polaron lifetimes are long at realistic magnetic fields (cf. Fig. 3). A rather unexpected effect is also related to the fact that increasing the electron-phonon coupling (the Fröhlich constant) broadens the anticrossing and thus strengthens the bottleneck mechanism [due to the exponential factor in Eq. (26)]. The efficiency of the bottleneck mechanism crucially depends, however, on the dot size (i.e.,

its confinement energy). The lifetime becomes very short when the confinement energy is close to the resonance with LO phonons (cf. inset in Fig. 3). Only when the confinement becomes stronger (approximately $\hbar\omega_0 > 40$ meV; cf. Fig. 2, inset) is the LO-TA channel excluded by energy conservation and the LO-LA channel is strongly suppressed due to the geometrical confinement effects (see Fig. 3, inset).

Finally, let us qualitatively describe the influence of real LO phonon dispersion on the results derived above. As was noticed above, the form factors governing the anharmonicity induced LO-TA process enforces $\boldsymbol{q} \approx -\boldsymbol{k}$ (this is similar to the bulk case[18]). Due to the decreasing k dependence of the LO phonon the total energy, $\Omega(\boldsymbol{k}) + \omega_{\mathrm{TA}}(-\boldsymbol{k})$ varies in a very small range. Therefore the relaxation window for LO-TA emission actually becomes more narrow. On the other hand, the energy difference between the LO and TA phonon varies in much wider range now; hence the process involving LO emission and TA absorption (at nonzero temperatures) is allowed in a wider range than estimated using the dispersionless model.

V. NUMERICAL VERIFICATION OF THE DAVYDOV METHOD ACCURACY

In this section we compare the spectrum found by the canonical transformation method with that obtained via exact numerical diagonalization of the Fröhlich interaction. It is now convenient to write the relevant electron and LO phonon terms of the Hamiltonian in the unperturbed, isotropic harmonic oscillator basis

$$H = \sum_{n=0,\pm 1} \epsilon_n^{(0)} a_n^\dagger a_n + W_\pm (a_+^\dagger a_- + a_-^\dagger a_+) + \hbar\Omega \sum_{\boldsymbol{k}} b_{\boldsymbol{k}}^\dagger b_{\boldsymbol{k}} + \frac{1}{\sqrt{N}} \sum_{nn'\boldsymbol{k}} F_{nn'}^{(\mathrm{o})}(\boldsymbol{k}) a_n^\dagger a_{n'} (b_{\boldsymbol{k}} + b_{-\boldsymbol{k}}^\dagger), \tag{27}$$

where we restricted the problem to the three lowest states, as in the previous sections, and $W_\pm$ is defined in Eq. (A1) in Appendix A.

As pointed out by Stauber, Zimmermann, and Castella[12] (SZC), the Fröhlich Hamiltonian (27) couples electronic states only with a very limited number of effective phononic modes. The symmetry of form factors (e.g., $\mathcal{F}_{0+1}^{(0)} = \mathcal{F}_{-10}^{(0)}$) reduces the number of these modes to 6. In order to simplify the further notation, we define the normalized coupling functions

$$\tilde{F}_0 = F_{11}^{\mathrm{o}(0)} / \sqrt{J_{11}^{(0)}}, \quad \tilde{F}_1 = F_{01}^{\mathrm{o}(0)} / \sqrt{J_{01}^{(0)}},$$

$$\tilde{F}_2 = F_{0-1}^{\mathrm{o}(0)} / \sqrt{J_{0-1}^{(0)}}, \quad \tilde{F}_3 = F_{1-1}^{\mathrm{o}(0)} / \sqrt{J_{1-1}^{(0)}},$$

$$\tilde{F}_4 = F_{-11}^{\mathrm{o}(0)} / \sqrt{J_{-11}^{(0)}}, \quad \tilde{F}_5 = F_{00}^{\mathrm{o}(0)} / \sqrt{J_{00}^{(0)}},$$

where the formulas for $F_{nn'}^{\mathrm{o}(0)}$ and $J_{nn'}^{(0)}$ (corresponding to the unperturbed basis) are obtained from Eqs. (4)–(6) and (18), respectively, by formally setting $\lambda = 0$, i.e., $c_+ = 1$, $c_- = 0$. With these definitions we have

$$\frac{1}{N} \sum_l |\tilde{F}_l(\boldsymbol{k})|^2 = 1.$$

Next, applying the SZC method to our three-level case, we define the annihilation operators

$$A_l = \frac{1}{\sqrt{N}} \sum_{\boldsymbol{k}} \tilde{F}_l(\boldsymbol{k}) b_{\boldsymbol{k}}.$$

The commutation relations for the new operators are

$$[A_l, A_{l'}] = 0, \quad [A_l^\dagger, A_{l'}^\dagger] = 0,$$

$$[A_l, A_{l'}^\dagger] = \frac{1}{N} \sum_{\boldsymbol{k}} \tilde{F}_l(\boldsymbol{k}) \tilde{F}_{l'}^*(\boldsymbol{k}).$$

Using the explicit formulas for $\tilde{F}_l$ for the parabolic dot one finds that the latter is non-zero only for $l = l'$, when it equals 1 by normalization, and for $l = 5$, $l' = 0$. Hence, the SZC orthonormalization is needed only for this pair of operators. The orthonormalized set of operators is given by

$$B_0 = \frac{A_0 - \sigma A_5}{\sqrt{1-\sigma^2}}, \quad B_l = A_l, \quad l = 1, \ldots, 5,$$

where

$$\sigma = [A_5, A_0^\dagger] = \frac{J_{00}^{(0)} - J_{01}^{(0)}}{\sqrt{J_{00}^{(0)} J_{01}^{(0)}}} = \frac{3}{\sqrt{11}}$$

(the final value uses the explicit form of the factors $J_{nn'}$ for the parabolic dot). According to the general theory,[12] the Hamiltonian may now be written as

$$H = \sum_{n=0,\pm 1} \epsilon_n^{(0)} a_n^\dagger a_n + W_\pm (a_+^\dagger a_- + a_-^\dagger a_+) + \hbar\Omega \sum_{l=0}^{5} B_l^\dagger B_l + [\sqrt{J_{00}} a_0^\dagger a_0 B_5 + \sqrt{J_{11}} (a_1^\dagger a_1 + a_{-1}^\dagger a_{-1})(\sigma' B_0 + \sigma B_5)$$
$$+ \sqrt{J_{01}} (a_0^\dagger a_1 + a_{-1}^\dagger a_0) B_1 + \sqrt{J_{01}} (a_0^\dagger a_{-1} + a_1^\dagger a_0) B_2 + \sqrt{J_{-11}} a_1^\dagger a_{-1} B_3 + \sqrt{J_{-11}} a_{-1}^\dagger a_1 B_4 + \mathrm{H.c.}],$$

where $\sigma' = \sqrt{1-\sigma^2}$.

The number of modes may be further reduced by one by defining the transformed modes

$$B_5' = \alpha B_5 + \beta B_0, \quad B_0' = \bar{\beta} B_5 - \bar{\alpha} B_0,$$

where

$$\beta = \frac{\sqrt{J_{00}^{(0)}/J_{11}^{(0)}} - \sigma}{\sigma'}, \quad |\alpha|^2 + |\beta|^2 = 1.$$

The simplest choice is $\alpha = \sqrt{2/3}$, $\beta = \sqrt{1/3}$. Upon this transformation, the phononic mode B_5' is coupled only to the electron number operator which commutes with the Hamiltonian and is constant in our restricted one-electron case. Hence, this mode may be suppressed and the reduced Fröhlich Hamiltonian reads(using the explicit values of coefficients)

$$H = \sum_{n=0,\pm 1} \epsilon_n^{(0)} a_n^\dagger a_n + W_\pm (a_+^\dagger a_- + a_-^\dagger a_+) + \hbar\Omega \sum_{l=0}^{4} B_l^\dagger B_l + \sqrt{J_{00}^{(0)}} \left\{ \frac{1}{\sqrt{3}} \left[a_0^\dagger a_0 + \frac{1}{4}(a_1^\dagger a_1 + a_{-1}^\dagger a_{-1}) \right] B_0 + \frac{1}{2}(a_0^\dagger a_1 + a_{-1}^\dagger a_0) B_1 \right.$$
$$\left. + \frac{1}{2}(a_0^\dagger a_{-1} + a_1^\dagger a_0) B_2 + \frac{\sqrt{3}}{4} a_1^\dagger a_{-1} B_3 + \frac{\sqrt{3}}{4} a_{-1}^\dagger a_1 B_4 + \text{H.c.} \right\},$$

The diagonalization of this Hamiltonian was performed numerically for the phononic occupation numbers limited to $0, \ldots, 3$. We have checked that allowing higher occupation numbers does not affect the obtained spectrum within the interesting energy range. The results, after deleting purely phononic modes (recognized by their weak dependence on the magnetic field[11]), are shown in Fig. 4.

We find out that the exact numerical diagonalization confirms the essential elements of the picture found by the Davydov method. For the lower resonance (between the "0" and "−" states) the coincidence between the two treatments is excellent, while for the other resonances, the exact behavior is reproduced with satisfactory accuracy, slightly decreased by the approximate methods of analytical solution of the Davydov equation (16).

The structure of the second-order resonance (at ~12 T) turns out to be more complicated. The resulting double-anticrossing structure is due to the overlap of the two resonances: the ground state with two phonons crosses the "+" state but also the "−" state with one phonon. The detailed structure of these resonances cannot be quantitatively accounted for by the analytical method because of the one-phonon approximations made in its derivation.

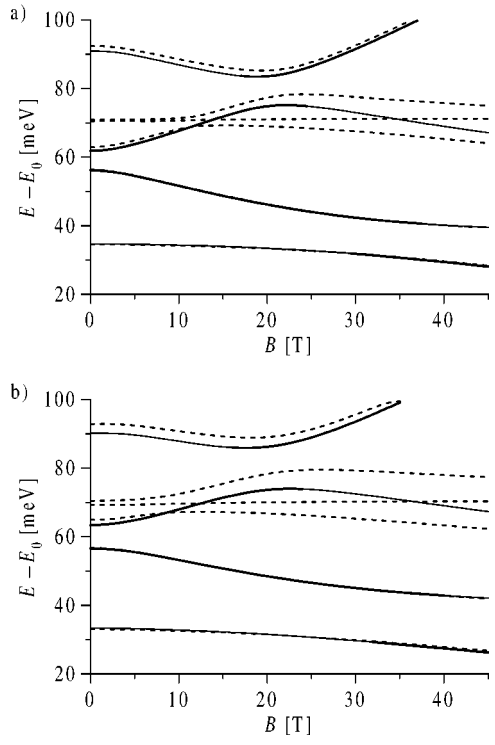

FIG. 4. Polaron spectrum in a weakly elliptical quantum dot in the presence of a magnetic field for (a) $\alpha = 0.07$ and (b) $\alpha = 0.15$. In both cases the approximate analytical results (solid lines) are compared to the exact numerical ones (dashed lines).

VI. CONCLUSIONS

The model of a weakly elliptical InAs/GaAs quantum dot was considered including coupling of electrons to bulk phonons in the presence of a magnetic field. The resulting magnetopolarons were analyzed in detail by application of the approximate Davydov diagonalization method. The accuracy of this method was further verified by exact numerical diagonalization of the relevant Fröhlich Hamiltonian. The obtained results are consistent with the experimental data in the magnetic field range where the latter are available.

Within the model three-level system, three polaron resonances were found, corresponding to the single- and two-phonon electron–LO-phonon interaction. Due to the anticrossing of electron levels in the vicinity of the LO phonon energy, the energy of polaronic states always differs from the LO phonon energy by a few meV. For a self-assembled dot with the electron excitation energy $\hbar\omega_0 \approx 58$ meV, only the second-order resonance lies within the range of easily accessible magnetic fields, although the most recent experiments[14] show also the existence of the first-order resonance at ~20 T.

The polaron spectra obtained here are consistent with the earlier results for GaAs-GaAlAs dots, both isotropic[9] and anisotropic[29,30] in plane. Astonishingly, including only 3D bulk modes results in being sufficient for reproducing the experimental data, contrary to the theoretical predictions.[7] This problem certainly deserves further study.

Another point of interest may be the dependence of the Huang-Rhys parameter $J_{nn}/(\hbar\Omega)^2$ on the dot size. In our model this parameter is proportional to $\omega^{1/2}$, i.e., to the inverse electron localization length [Eqs. (17) and (18)]. This constitutes an essential difference between the interaction with bulk phonons and with the confined phonons, as in the case of semiconductor nanospheres in glass.[31] In the latter case, no size dependence was observed which was attributed to the confinement of the vibrational wave functions. In fact, in the Ref. 31 excitonic polarons were analyzed, while the present study focuses on a single excess electron. Nevertheless, we do not expect a much different size dependence in the excitonic case.[32]

Two channels of polaron relaxation by phonon emission (at low temperatures) were studied. The first one results from the direct electron–LA-phonon coupling via the deformation potential. As the single-LA-phonon transition in a typical InAs/GaAs dot is forbidden by energy conservation, the only relevant process is the resulting two-phonon LO-LA emission. This process involves the electron–LA-phonon interaction and is therefore affected by the bottleneck effect, similarly as in the single-phonon case. In a 60 meV dot, this process is practically totally suppressed for reasonable magnetic fields. Although it might play some role in the case of a weaker lateral confinement, due to wide anticrossing of levels at the resonances, the corresponding relaxation times are always longer than a picosecond.

The second relaxation channel is due to the phonon anharmonicity, which leads to the decay of a LO phonon into another LO phonon and a TA phonons. This also leads to a two-phonon process, involving the LO and TA phonon. In this case, however, the resulting amplitude *does not* involve the electron–TA-phonon coupling and therefore is not affected by the bottleneck mechanism. In fact, unlike in the previous case, the relaxation time with respect to this process decreases with increasing energy gap. This is essentially due to different dependence of the relaxation probabilities (24) and (25) on the acoustical phonon wave vector q for various channels. On the other hand, the energies of the TA phonons in GaAs are limited to a relatively narrow band and this relaxation channel is likely to be forbidden in a self-assembled dot by energy conservation, even for realistic dispersion of LO phonons. In a model with realistic phonon dispersion curves this restriction is stronger for TA phonon emission while it is released for TA phonon absorption (possible at higher temperatures),

Thus, the bottleneck effect and the energy conservation open windows of inefficiency of relaxation processes. As the relaxation times can be treated as the upper limit for the overall decoherence times,[33,34] these inefficiency windows may be useful for semiconductor-based quantum information processing purposes. This conclusion is also confirmed by recent experimental data, showing nanosecond dephasing times in GaAs quantum dots.[35] However, some further investigation is still needed, involving, e.g., the analysis ofthe relaxation at finite temperatures and the rate of pure dephasing processes (which seems to be of a comparable order as the relaxation rate[36]).

ACKNOWLEDGMENTS

L.J. and P.M. are indebted to Professor H. Konwent for valuable discussions. This work was supported by E.E.C. Project No. IST-1999-11311 (SQID) and KBN Project No. PB 2 PO3B 055 18.

APPENDIX A: ELECTRON EIGENSTATES IN THE WEAKLY ELLIPTICAL DOT

The first excited state is distant from the ground state in the quantum dot with $\hbar\omega_0$ not small; hence the correction to the energy, due to the W term, may be calculated in the first order of the perturbation. For the ground state we have

$$\Delta\epsilon_0 = \int d^2r_\perp |\psi_0(\boldsymbol{r}_\perp)|^2 W(\boldsymbol{r}_\perp) = 0$$

and the wave function may be taken in the zeroth order. In order to take into account the closeness of the levels $m = \pm 1$ (degenerated at $B=0$ and $\lambda=0$), we perform the diagonalization in the corresponding two-dimensional subspace. The coefficients in Eqs. (2d) and the energy eigenvalues (2c) are found from the equation

$$\begin{pmatrix} \epsilon_{+1}^{(0)} + W_{++} - \epsilon & W_{+-} \\ W_{-+} & \epsilon_{-1}^{(0)} + W_{--} - \epsilon \end{pmatrix} \begin{pmatrix} c_1 \\ c_2 \end{pmatrix} = 0,$$

where $\epsilon_{\pm 1}^{(0)} = 2\hbar\omega \mp \frac{1}{2}\hbar\omega_c$ are the unperturbed energies of the $m=\pm 1$ states and W_{ij} are the matrix elements of the perturbation,

$$W_{\pm\pm} = \int d^2r_\perp |\psi_{\pm 1}(\boldsymbol{r}_\perp)|^2 W(\boldsymbol{r}_\perp) = 0$$

and

$$\begin{aligned} W_{\pm\mp} &= \int d^2r_\perp \psi_{\pm 1}^*(\boldsymbol{r}_\perp) W(\boldsymbol{r}_\perp) \psi_{\mp 1}(\boldsymbol{r}_\perp) \\ &= \frac{\lambda}{2} m^* \omega_0^2 \int_0^{2\pi} d\theta \cos 2\theta e^{\mp 2\theta} \frac{1}{\pi l_B^4} \int_0^\infty r dr r^4 e^{-(r/l_B)^2} \\ &= \frac{\lambda}{2} \hbar \frac{\omega_0^2}{\omega} \approx \frac{\lambda}{2} \hbar\omega_0, \end{aligned} \tag{A1}$$

where the final approximation is valid for $\omega_c \ll \omega_0$.

APPENDIX B: FRÖHLICH CONSTANT FOR ELECTRONS CONFINED IN THE QUANTUM DOT

The dimensionless parameter, called the Fröhlich constant, is defined as follows:

$$\alpha = \frac{e^2}{\tilde{\epsilon}} \sqrt{\frac{m^*}{2\hbar^3\Omega}}. \tag{B1}$$

If we take (as for bulk GaAs) $\epsilon_0 = 12.9$, $\epsilon_\infty = 10.9$, $m^* = 0.067 m_e$, and $\hbar\Omega = 36$ meV, then $\alpha = 0.071$, and this value has been verified experimentally in bulk GaAs.[37] However, for electrons confined on the nanometer scale, as in the

InAs/GaAs self-assembled dot with a radius of the order of 10 nm, the recent experimental data on far-infrared attenuation[11] indicated that $\alpha \approx 0.15$.

The enhancement of the electron–LO-phonon interaction for QD's manifests itself also via a significant increase of the Huang-Rhys factor[38] for satellite LO-phonon-assisted photoluminescence features in III-V quantum dots (InAs/GaAs),[39–41] as well as in spherical nanocrystals II-VI.[42] This phenomenon concerns the exciton–LO-phonon interaction and the geometrical separation of *e-h* charges in localized exciton states turns out to be insufficient[39,41] to explain it. Some effects beyond *e-h* charges separation were invoked, for spherical II-VI dots, the nonadiabaticity,[42] and for pyramid-shaped III-V, InAs/GaAs dots, piezoelectricity.[41]

In view of the FIR experimental data[11] suggesting an increase of the Fröhlich constant α, one can attempt to interpret this effect in phenomenological terms using description by *inertial* and *noninertial* parts of local crystal polarization.[16] For the electron–LO-phonon interaction important is only an *inertial* part of the local polarization. The *noninertial* part, accompanying the moving electrons, is included into the crystal field which defined both the electron and phonon states. Therefore, the *inertial* polarization of the crystal acting on the free lattice electrons equals $\mathbf{P}(\mathbf{r}) = \mathbf{P}_0(\mathbf{r}) - \mathbf{P}_\infty(\mathbf{r})$, where $\mathbf{P}_0 = [(\epsilon_0 - 1)/4\pi\epsilon_0]\mathbf{D}$ and $\mathbf{P}_\infty = [(\epsilon_\infty - 1)/4\pi\epsilon_\infty]\mathbf{D}$ ($\mathbf{D}$ is the electrical induction) are the static and the high-frequency (of atomic-scale) polarizations, respectively. This formula leads, in a standard manner, to the Fröhlich constant given by Eq. (B1).[16]

For the localized electron in a QD, the *inertial* part of the polarization is greater in comparison with the free-moving lattice electron since the quasiclassical velocity of the confined electron ($\sim \hbar/m^* d$) is greater than the velocity of the conducting band electrons (especially near the Γ point). The *inertial* part of polarization acting on electron quickly moving within the dot can thus be written in the form $\mathbf{P}'(\mathbf{r}) = \mathbf{P}_0(\mathbf{r}) - \eta\mathbf{P}_\infty(\mathbf{r})$, with some factor $0 \leqslant \eta \leqslant 1$, depending on the localization scale (given by d, the diameter of the dot). It is clear that $\eta = 1$ when $d \to \infty$ and $\eta = 0$ when d attains dimensions of atoms, i.e., when $d \sim a$ (a, the diameter of a unit cell). Therefore, within the linear approximation with respect to the small parameter a/d (or, equivalently, linear with respect to the quasiclassical velocity of the confined electron), $\eta = (d-a)/d$. Hence for the confined electron we have $\mathbf{P}'(\mathbf{r}) = D/(4\pi\tilde{\epsilon}')$, where $1/\tilde{\epsilon}' = (1 - a/d)/\epsilon_\infty - 1/\epsilon_0 + a/d$. This formula leads to the renormalized Fröhlich constant in the form

$$\alpha' = \frac{e^2}{\tilde{\epsilon}'}\sqrt{\frac{m^*}{2\hbar^3\Omega}}. \tag{B2}$$

For QD with $d \approx 25$ nm, as was reported in Ref. 11, we have $d \approx 40a$ (for GaAs, $a \simeq 0.56$ nm), which yields the desired value the of the Fröhlich constant: $\alpha' \approx 0.15$. The formula (B2) would also be helpful for understanding of the enhancement of the Huang-Rhys parameter,[39,40,42,41] which scales as α (some further corrections result from the different Fröhlich constants for electrons and holes due to the distinct effective mass). For dots of diameter of ~ 5–9 nm, as reported in Ref. 39, the corresponding $\alpha' \sim 0.4$–0.3, and for dots with diameter ~ 15–19 nm (cf. Ref. 41), $\alpha' \sim 0.25$–0.18. In the former case it gives the factor of 6–5 and in the latter 4–3 for the Huang-Rhys parameter, which coincide well with experimental data.[39,41]

An additional small renormalization of the Fröhlich constant can also be connected with a change of the effective mass due to localization and strain effects in InAs/GaAs dot. It was theoretically estimated[43] that for the strain-induced InAs/GaAs QD, similar in size as discussed above, the effective mass $\simeq 0.05 m_e$. However, this correction does not cause any significant change in α as the shift from the bulk value, $\simeq 0.06 m_e$, is rather small. Additionally, $\alpha \propto \sqrt{m^*}$, resulting in renormalization factor of ~ 0.9.

*On leave from Institute of Physics, Odessa University, Ukraine.

[1] M. Grundmann, Physica E (Amsterdam) **5**, 167 (2000); S. Fafard, K. Hinzer, S. Raymond, M. Dion, J. Mc. Caffrey, Y. Feng, and S. Charbonneau, Science **274**, 1350 (1996).

[2] D. Loss and D. P. DiVincenzo, Phys. Rev. A **57**, 120 (1998); Ch. Bennet and D. DiVincenzo, Nature (London) **404**, 247 (2000).

[3] P. Zanardi and F. Rossi, Phys. Rev. B **59**, 8170 (1999); E. Biolatti, R. C. Iotti, P. Zanardi, and F. Rossi, Phys. Rev. Lett. **85**, 5647 (2000).

[4] J. M. Kikkawa and D. D. Awschalom, Phys. Rev. Lett. **80**, 4313 (1998).

[5] For a review, see, e.g., L. Jacak, P. Hawrylak, and A. Wojs, *Quantum Dots* (Springer-Verlag, Berlin, 1998).

[6] A. Wójs, P. Hawrylak, S. Fafard, and L. Jacak, Phys. Rev. B **54**, 5604 (1996).

[7] M. H. Degani and G. A. Farias, Phys. Rev. B **42**, 11 950 (1990).

[8] K. D. Zhu and S. W. Gu, Phys. Lett. A **163**, 435 (1992).

[9] L. Wendler, A. V. Chaplik, R. Haupt, and O. Hipólito, J. Phys.: Condens. Matter **5**, 8031 (1993).

[10] A. Chatterjee and S. Mukhopadhyay, Acta Phys. Pol. B **32**, 473 (2001).

[11] S. Hameau, Y. Guldner, O. Verzelen, R. Ferreira, G. Bastard, J. Zeman, A. Lemaître, and J. M. Gerard, Phys. Rev. Lett. **83**, 4152 (1999).

[12] T. Stauber, R. Zimmermann, and H. Castella, Phys. Rev. B **62**, 7336 (2000).

[13] T. Inoshita and H. Sakaki, Phys. Rev. B **56**, R4355 (1997).

[14] S. Hameau, J. N. Isaia, Y. Guldner, E. Deleporte, O. Verzelen, R. Ferreira, G. Bastard, J. Zeman and J. M. Gerard, Phys. Rev. B **65**, 085316 (2002).

[15] A. Davydov and G. Pestryakov, Phys. Status Solidi B **49**, 505 (1972).

[16] A. Davydov, *Solid State Theory* (Nauka, Moscow, 1976) (in Russian).

[17] L. Jacak, J. Krasnyji, D. Jacak, and P. Machnikowski, Phys. Rev. B **65**, 113305 (2002).

[18] F. Vallée and F. Bogani, Phys. Rev. B **43**, 12 049 (1991); F. Vallée, *ibid.* **49**, 2460 (1994).

[19] K. Huang and A. Rhys, Proc. R. Soc. London, Ser. A **204**, 406 (1950).

[20] D. J. Mowbray *et al.*, Acta Phys. Pol. B **98**, 279 (2000).
[21] C. Pryor, Phys. Rev. B **57**, 7190 (1998).
[22] M. Korkusiński and P. Hawrylak, Phys. Rev. B **63**, 195311 (2001).
[23] E. Lifshitz and L. Pitaevskii, *Physical Kinetics* (Butterworth-Heinemann, Oxford, 1997).
[24] D. Strauch and B. Dorner, J. Phys.: Condens. Matter **2**, 1457 (1990).
[25] *Handbook of Mathematical Functions* Natl. Bur. Stand. Appl. Math. Ser. No. 55, edited by M. Abramovitz and I. A. Stegun (U.S. GPO, Washington, D.C., 1965).
[26] U. Bockelmann and G. Bastard, Phys. Rev. B **42**, 8947 (1990).
[27] T. Inoshita and H. Sakaki, Phys. Rev. B **46**, 7260 (1992).
[28] O. Verzelen, R. Ferreira, and G. Bastard, Phys. Rev. B **62**, R4809 (2000).
[29] R. Haupt and L. Wendler, Physica B **184**, 394 (1993).
[30] R. Haupt and L. Wendler, Solid-State Electron. **37**, 1153 (1994).
[31] M. C. Klein, F. Hache, D. Ricard, and C. Flytzanis, Phys. Rev. B **42**, 11 123 (1990).
[32] L. Jacak, P. Machnikowski, J. Krasnyj, and P. Zoller, Eur. Phys. J. D. (to be published).
[33] D. Bouwmeester, A. Eckert, and A. Zeilinger, *The Physics of Quantum Information* (Springer-Verlag, Berlin, 2000).
[34] J. Preskill, Quantum Information and Computation, http://www.theory.caltech.edu/~preskill/ph229.
[35] P. Borri, W. Langbein, S. Schneider, U. Woggon, R. L. Sellin, D. Ouyang, and D. Bimberg, Phys. Rev. Lett. **87**, 157401 (2001).
[36] B. Krummheuer, V. M. Axt, and T. Kuhn, Phys. Rev. B **65**, 195313 (2002).
[37] S. Adachi, J. Appl. Phys. **58**, R1 (1985).
[38] K. Huang and A. Rhys, Proc. R. Soc. London, Ser. A **204**, 406 (1950).
[39] A. García-Cristóbal, A. W. Minnaert, V. M. Fomin, J. T. Devreese, A. Yo. Silov, J. E. M. Haverkort, and J. H. Wolter, Phys. Status Solidi B **215**, 331 (1999).
[40] A. Lemaître, A. D. Ashmore, J. J. Finley, D. J. Mowbray, M. S. Skolnick, M. Hopkinson, and T. F. Krauss, Phys. Rev. B **63**, 161309(R) (2001).
[41] R. Heitz, I. Mukhametzhanov, O. Stier, A. Madhukar, and D. Bimberg, Phys. Rev. Lett. **83**, 4654 (1999).
[42] V. M. Fomin, V. N. Gladilin, J. T. Devreese, E. P. Pokatilov, S. N. Balaban, and S. N. Klimin, Phys. Rev. B **57**, 2415 (1998).
[43] C. Pryor, Phys. Rev. Lett. **80**, 3579 (1998).